Supplementary Information (SI) for

[Unraveling El Niño's Impact on the East Asian Monsoon and Yangtze River Summer Flooding]

Wenjun Zhang[1], Fei-Fei Jin[2,3], Malte F. Stuecker[2], Andrew T. Wittenberg[4], Axel Timmermann[5], Hong-Li Ren[3], Jong-Seong Kug[6], Wenju Cai[7], Mark Cane[8]

[1]*CIC-FEMD/ILCEC, Key Laboratory of Meteorological Disaster of Ministry of Education (KLME), Nanjing University of Information Science and Technology, Nanjing, China*

[2]*Department of Atmospheric Sciences, SOEST, University of Hawai'i at Mānoa, Honolulu, HI, USA*

[3]*Laboratory for Climate Studies, National Climate Center, China Meteorological Administration, Beijing, China*

[4]*National Oceanic and Atmospheric Administration, Geophysical Fluid Dynamics Laboratory, Princeton, NJ, USA*

[5]*IPRC, SOEST, University of Hawai'i at Mānoa, Honolulu, HI, USA*

[6]*School of Environmental Science and Engineering, Pohang University of Science and Technology (POSTECH), Pohang, South Korea*

[7]*CSIRO Oceans and Atmosphere, Aspendale, Victoria, Australia*

[8]*Lamont-Doherty Earth Observatory of Columbia University, USA*

Geophysical Research Letters

Table S1. Definitions of different SST anomaly (SSTA) indices used in this study.

Index Name	Definition
El Niño Modoki index (EMI)[1]	$EMI=[SSTA]_C-0.5[SSTA]_E-0.5[SSTA]_W$, where the brackets represent the area-averaged SSTA over the regions C (10°S–10°N, 165°E–140°W), E (15°S–5°N, 110°W–70°W), and W (10°S–20°N, 125°E–145°E)[1]
C-index[2]	*C-index*=(PC1+PC2)/$2^{(1/2)}$, where the PCs (normalized and 1-2-1 filter applied) correspond to the EOFs of the SST anomalies over the tropical Pacific (10°S–10°N, 110°E–60°W)[2]
Trans-Niño index (TNI)[3]	Difference between normalized SSTA over regions Niño4 (5°S–5°N, 160°E–150°W) and Niño1+2 (0°–10°S, 80°–90°W)[3]
Indian Ocean Dipole (IOD)[4]	SSTA difference between the western (50°E–70°E, 10°S–10°N) and southeastern (90°E–110°E, 10°S –0°) tropical Indian Ocean[4]
Indian Ocean Basin Mode (IOBM)[5]	SSTA over the tropical Indian Ocean (20°S–20°N, 40°–100°E)[5]
SSTA dipole pattern between the Indian Ocean and the WNP (IO_WNP)[6]	SSTA difference between the IO (10°S–10°N, 50°E–110°E) and the WNP (0°–15°N, 120°E–160°E)[6]

References for definitions of different SSTA indices

1. Ashok, K., Behera, S. K., Rao, S. A., Weng, H. Y. & Yamagata, T. El Niño Modoki and its possible teleconnection. *J. Geophys. Res.* **112**, C11007 (2007).
2. Takahashi, K., Montecinos, A., Goubanova, K. & Dewitte B. ENSO regimes: Reinterpreting the canonical and Modoki El Niño. *Geophys. Res. Lett.* **38**, L10704 (2011).
3. Trenberth, K. E. & Stepaniak, D. P. Indices of El Niño evolution. *J. Climate* **14**, 1697–1701 (2001).
4. Saji, N. H., Goswami, B. N., Vinayachandran, P. N., & Yamagata, T. A dipole in the tropical Indian Ocean. *Nature* **401**, 360–363 (1999).
5. Xie, S. P., Hu, K., Hafner, J., Tokinaga, H., Du, Y., Huang, G. & Sampe, T. Indian Ocean capacitor effect on Indo-Western Pacific climate during the summer following El Niño. *J. Climate* **22**, 730–747 (2009).
6. Wang, B., Xiang, B. & Lee, J.-Y. Subtropical High predictability establishes a promising way for monsoon and tropical storm predictions. *Proc. Natl. Acad. Sci. USA* **110**, 2718–2722 (2013).

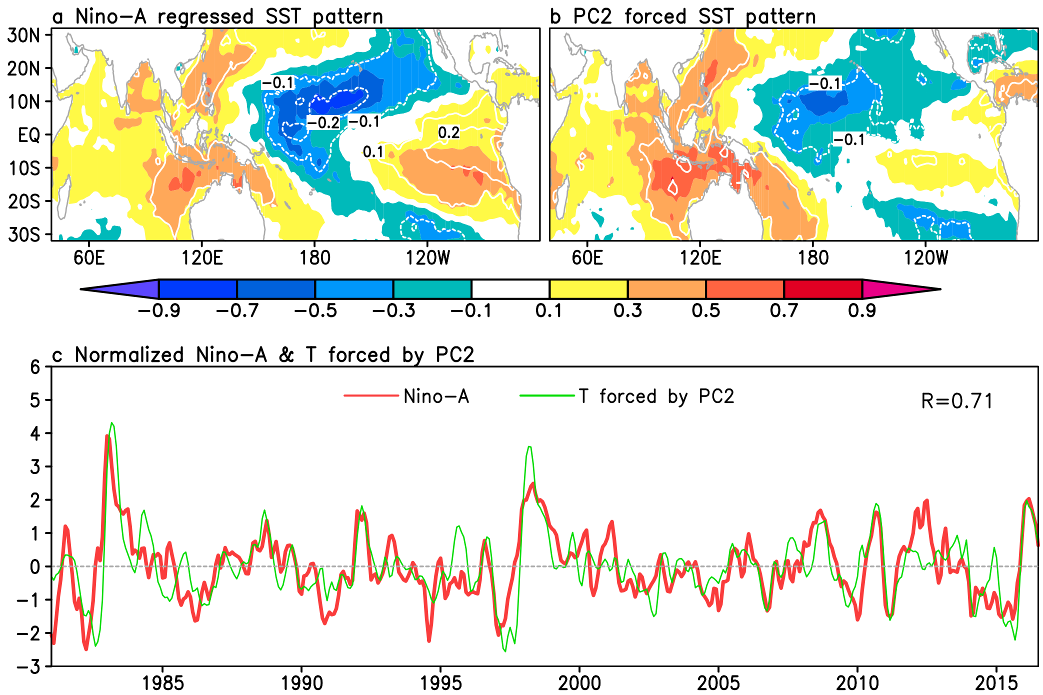

Figure S1. Spatial and temporal patterns associated with the Niño-A index and SST anomaly time series (T) forced by the second principal component (PC2)-associated surface wind anomalies based on the equation $dT/dt + \lambda T = \beta(PC2)_N$ (see Methods section). (**a and b**) Regressed SST anomalies (contour; °C) with respect to Niño-A (a) and T (b). Shading indicates the correlation coefficient with SST anomalies. The contour interval is 0.1 °C. **(c)** Normalized Niño-A (same plot as Fig. 2d) and T time series.

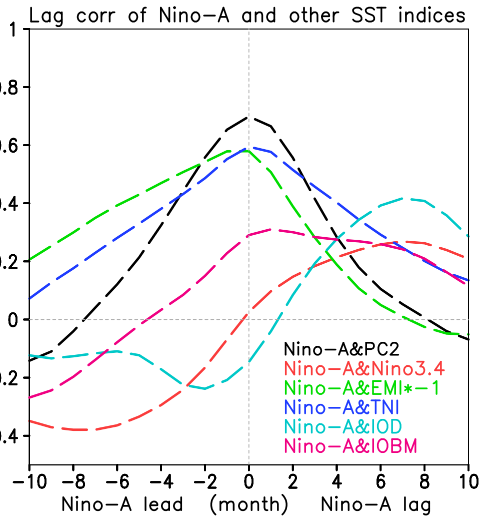

Figure S2. Lead/lag correlation between the Niño-A index and PC2, Niño3.4, EMI (reversed sign), TNI, IOD, and IOBM indices over the period of 1979–2015. Negative lags (months) means that Niño-A is leading the other indices

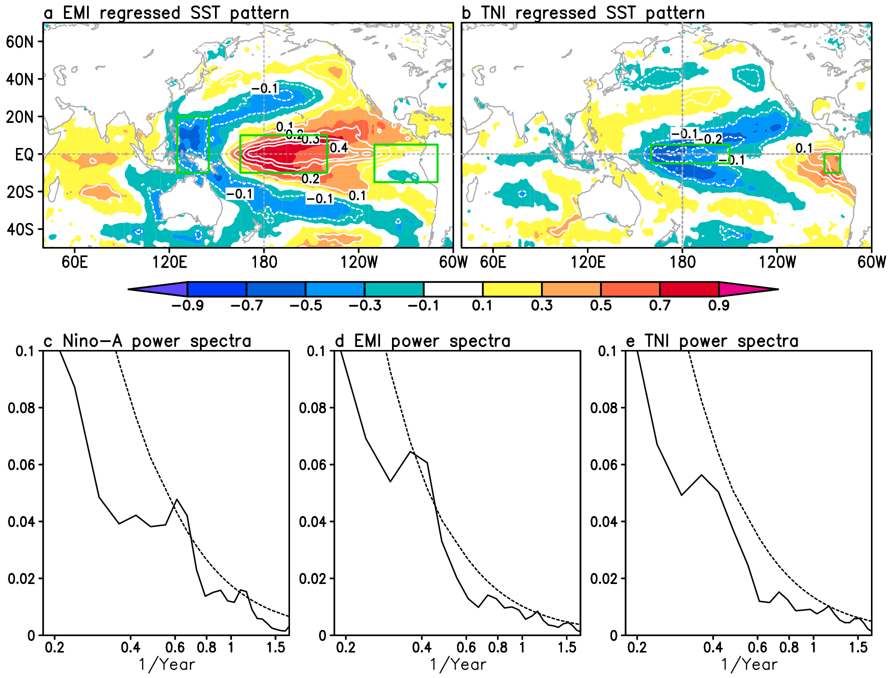

Figure S3. **(a and b)** Spatial SST anomaly patterns (contour, °C) for the EMI (a) and TNI (b). Shading indicates the correlation coefficient with SST anomalies. **(c-e)** Power spectra of Niño-A (c), EMI (d), and TNI (e) over the period of 1979-2012. The dashed line represents the 95% confidence interval of a χ^2 test against AR(1).

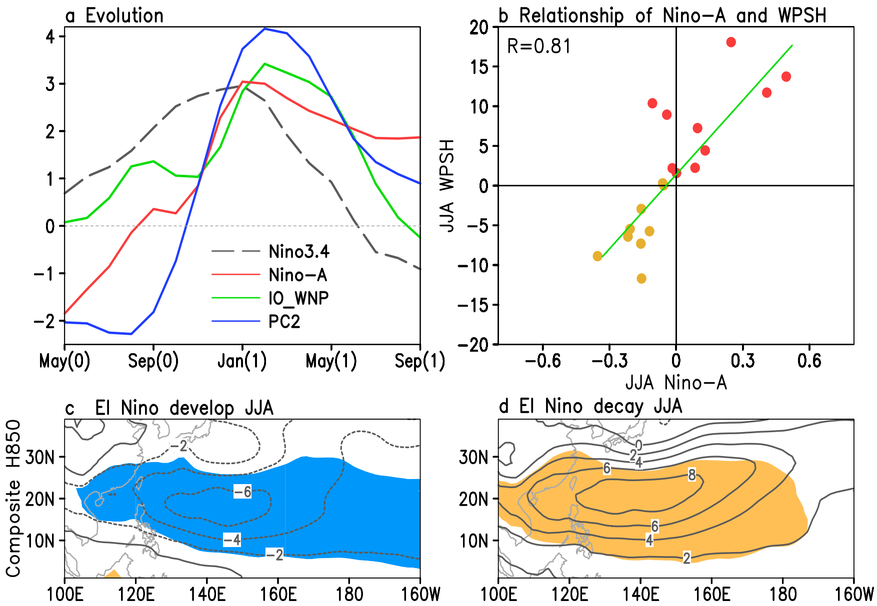

Figure S4. **(a)** Composite evolution of two strong El Niño events (1982/83 and 1997/98) for the normalized PC2, Niño3.4, Niño-A, and IO_WNP indices. The El Niño developing year and the decaying year are designated as 0 and 1, respectively. **(b)** Scatter diagram of boreal summer (JJA) Niño-A (normalized) and WPSH indices (m) during El Niño years (1982/83, 1986/87, 1991/92, 1994/95, 1997/98, 2002/03, 2004/05, 2006/07, 2009/10). Yellow and red colors represent the developing and decaying summers, respectively. **(c and d)** Composite geopotential height anomalies (contour, m) at 850 hPa during El Niño developing (c) and decaying (d) summers. Shading indicates significance at the 95% confidence level.

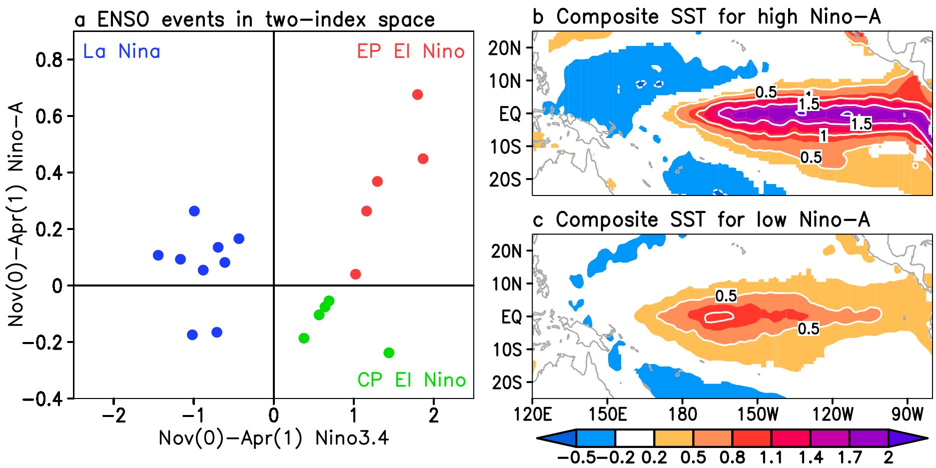

Figure S5. **(a)** Scatter diagram of the Niño3.4 and Niño-A indices (°C) during the ENSO mature phase averaged from November (0) to April (1). **(b and c)** Composite SST anomalies (contour and shading, °C) for the high (b, red dots in a) and low (c, green dots in a) Niño-A values during El Niño mature phase. Only values above the 95% confidence level are shown.

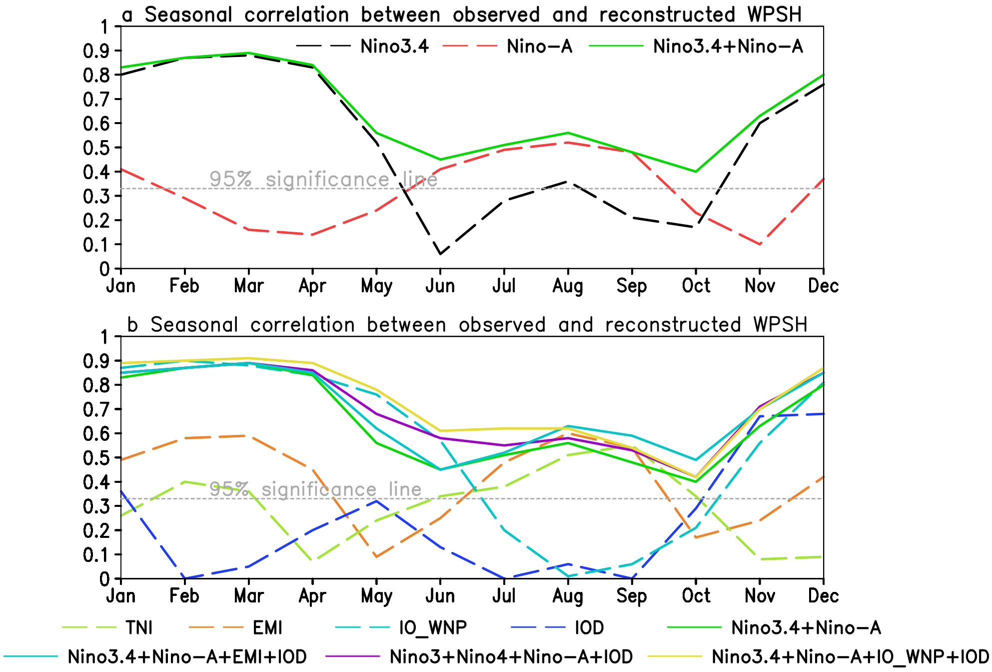

Figure S6. **(a)** Seasonal (3-month running mean) correlations for an East Asia monsoon index (WPSH) with Niño3.4, Niño-A, and their combination. **(b)** Same as (a) but for other indices (Table S1).

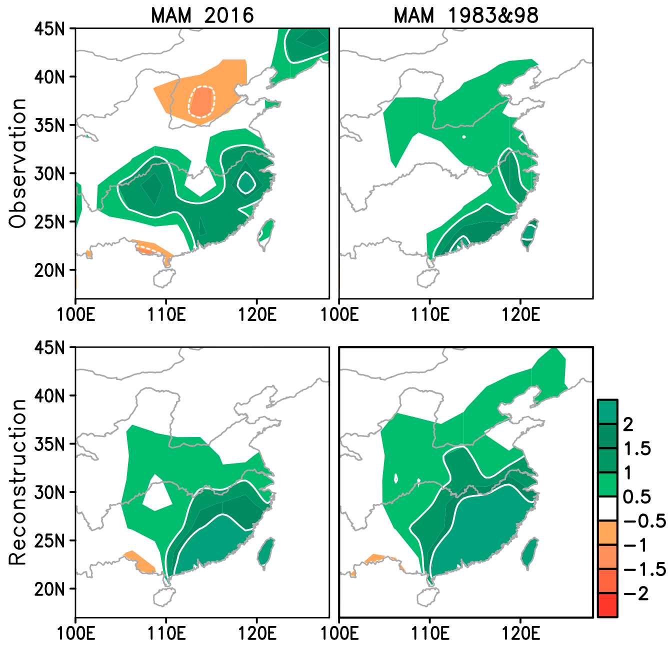

Figure S7. Observed and reconstructed precipitation anomalies (shading in mm/d and contour interval 1 mm/d) during boreal spring (MAM) of 2016 (left column) and the average of MAM 1983 and MAM 1998 (right column). The reconstruction uses the linear regression with the Niño3.4 and Niño-A indices.